Longitudinal excitations in $Mg_{70}Zn_{30}$ glass

1999 J. Phys.: Condens. Matter 11 7079

(http://iopscience.iop.org/0953-8984/11/37/305)

J. Phys.: Condens. Matter **11** (1999) 7079–7088. Printed in the UK PII: S0953-8984(99)02452-2

Longitudinal excitations in $Mg_{70}Zn_{30}$ glass

C J Benmore†‡, S Sweeney†, R A Robinson§, P A Egelstaff† and J-B Suck‖

† Department of Physics, University of Guelph, Guelph, Ontario N1G 2W1, Canada
‡ ISIS Facility, Rutherford Appleton Laboratory, Chilton, Oxfordshire OX11 OHR, UK
§ Los Alamos National Laboratory, LANSCE, Los Alamos, NM 87545, USA
‖ Institute of Physics, Materials Research and Liquids, TU Chemnitz, D-09107 Chemnitz, Germany

Received 9 March 1999, in final form 16 June 1999

Abstract. The Neutron Brillouin Scattering technique has been used to measure longitudinal excitations in a magnesium–zinc glass at momentum transfers, Q, within the first pseudo-Brillouin zone. The measurements were performed at room temperature and at constant momentum transfer, down to $Q = 6.2$ nm^{-1}, and an energy transfer of $E = 16$ meV. The experimental one-phonon spectral functions for the glass have been extracted and compared directly to theoretical predictions. At the first Brillouin zone boundary ($Q_P/2 = 13$ nm^{-1}) experiment and theory show some agreement, but at lower momentum transfers there is a shift of several meV in the peak position of the neutron intensity, towards lower energies. Evidence for the two observed modes is presented and the possibility of mode mixing is discussed. In conclusion, the need for new simulations is highlighted.

1. Introduction

The investigation of properties of elementary collective excitations such as phonons and magnons in glasses using neutron scattering techniques can provide information that is directly comparable to theory. In particular, neutron inelastic scattering measurements made at momentum transfers $\hbar Q$ within the first pseudo-Brillouin zone, a technique known as Neutron Brillouin Scattering (NBS), can be used to measure the dynamical structure factor where the dispersion of such excitations may be observed [1–6]. Here $\hbar Q$ is the momentum transfer in a scattering experiment. Generally, inelastic scattering experiments on crystals are performed in higher-order Brillouin zones in order to gain intensity, and the results are presented after reduction to the first zone. In disordered materials, however, this is considerably more difficult, as there is no reciprocal lattice. Nonetheless, provided these systems have short and/or medium range order, low-order pseudo-Brillouin zones can be defined close to the origin of reciprocal space. Here, the first maximum Q_P in the static structure factor $S(Q)$ can be regarded as the first broadened reciprocal lattice point, such that the first pseudo-Brillouin zone extends up to $Q_P/2$ in reciprocal space [1, 2].

Information on the collective dynamics in liquids and amorphous materials is typically obtained through the extraction of single-excitations (phonons in harmonic solids), represented by $S_1(Q, \omega)$, from the measured dynamic structure factor $S(Q, \omega)$, where $\hbar\omega$ is the experimentally observed energy transfer. This is because the peaks in $S_1(Q, \omega)$, which contain information on the dynamical modes of the system, are more easily accessible to theoretical analysis and more reliably interpreted than structure in $S(Q, \omega)$ itself. As Q is increased beyond the first pseudo-Brillouin zone these peaks become less pronounced, and at $Q > 2Q_P$

0953-8984/99/377079+10$30.00

the structure of $S(Q, \omega)$ is dominated by the vibrational density of states, describing single particle motion [1–3].

Strictly speaking, neutrons only couple directly to the longitudinal vibrations within the first Brillouin zone and to transverse vibrations via Umklapp type processes outside the first Brillouin zone. This provides a tool in NBS experiments for distinction between longitudinal and transverse excitations; however, due to the nature of disordered systems it has been suggested that some mixing of modes may occur [7]. NBS experiments impose uncompromising kinematic constraints on a spectrometer, since they require a sufficiently large ω-range at the smallest Q values. A full picture of the dispersion curve demands the use of high energies for the incident neutrons at scattering angles close to the straight-through beam, where there are a large amount of associated background and multiple scattering events [8].

The metallic glass $Mg_{70}Zn_{30}$ can be melt spun in continuous ribbons, from which a suitable neutron scattering specimen may be made. Since the scattering amplitudes for Mg and Zn are similar (5.38 and 5.69 fm, respectively) and the coherent scattering is about 98% of the total, this is a suitable sample for the investigation of collective excitations. We may represent, therefore, the scattering cross section by an approximate formula, using S for the average of Mg and Zn,

$$\frac{\mathrm{d}^2\sigma}{\mathrm{d}\Omega/\mathrm{d}\omega} = \bar{b}^2 \left(\frac{\underline{k}}{\underline{k}_0}\right) S(Q, \omega) \tag{1}$$

where $\bar{b}$ is the average scattering amplitude for Mg and Zn. $\underline{k}_0$ and $\underline{k}$ are the incident and scattered wavevectors, respectively. Moreover, this metallic glass has been the subject of investigation in previous experimental studies with momentum transfer values down to 8 nm^{-1} at energy transfers of 25 meV [1–6]. We note that the first pseudo-Brillouin zone boundary $Q_P/2$ is at 13 nm^{-1} for glassy $Mg_{70}Zn_{30}$. In addition, there are extensive computer simulations using *a priori* potentials and other theoretical work [9].

Previous experimental and theoretical work on this glass has demonstrated that general features of the dispersion curves for the longitudinal modes are in approximate agreement. However, whilst the measurements have been performed at a constant angle the calculations have been made at constant Q. The intention of this paper is to present our NBS results for glassy $Mg_{70}Zn_{30}$ in which the accessible Q-range is well inside the first pseudo-Brillouin zone and the data are taken at constant momentum transfer rather than constant angle. The improved resolution data measured at the lowest momentum transfers provide an accurate measurement of the energy dispersion of the main phonon intensity. To achieve this experimentally it is necessary to use a relatively high incident energy (0.184 eV or a neutron velocity of 6000 m s^{-1}), so that the neutron velocity will be greater than the velocity of sound, and scattering angles will be as low as 1°. In addition, a high energy resolution is required under these conditions. A further goal of this experiment was to examine the spectral shape of the longitudinal modes as Q is decreased. These new data are compared to existing theoretical predictions [9].

2. Theoretical background

It is the structure (peaks and shoulders) of the single-excitation part $S_1(Q, \omega)$ of the dynamic structure factor $S(Q, \omega)$ (equation (1)) that contains important information about the collective dynamics of the atoms. Thus, we separate this function into three parts as:

$$S(Q, \omega) = S_0(Q, \omega) + S_1(Q, \omega) + S_m(Q, \omega) \tag{2}$$

where S_0 represents the elastic scattering, S_1 the single-excitation component and S_m multiple-excitation contribution. The smallest Q-values which can be reached in an NBS experiment

at a given ω depend on the scattering angle θ and the incident energy E_0 necessary for the excitation of the modes. These quantities are related by the conditions for conservation of momentum and energy, namely,

$$Q^2 = k_0^2 + k^2 - 2kk_0\cos\theta \qquad \text{and} \qquad \omega = \frac{\overline{h}}{2m}(k_0^2 - k^2) \tag{3}$$

where m is the neutron mass and k and k_0 are the moduli of the neutron wave vector mentioned above. By eliminating k, these equations become:

$$\overline{h}Q = [2m(E_0 - \overline{h}\omega) - 2\sqrt{E_0(E_0 - \overline{h}\omega)}\cos\theta]^{1/2}. \tag{4}$$

In this section we assume the experimental conditions are such that these equations yield values in the first pseudo-Brillouin zone of the $Mg_{70}Zn_{30}$ glass.

If we consider $S_1(Q,\omega)$ for a simple isotropic polycrystal with atomic mass M, the single longitudinal excitation scattering in the first Brillouin zone [10] can be written as:

$$S_1(Q,\omega) - \mathrm{e}^{-2W}\mathrm{e}^{(-\overline{h}\omega/k_BT)}[A\delta(Q-q)\delta(\omega-\omega_q)\rho(\omega_q)] \tag{5}$$

where

$$A = \frac{\overline{h}^2Q^2\mathrm{e}^{(-\overline{h}\omega/k_BT)}}{6M\omega(1-\mathrm{e}^{(-\overline{h}\omega/k_BT)})}$$

e^{-2W} is the Debye–Waller factor, (q,ω_q) are the wave number and frequency of a longitudinal phonon in the first Brillouin zone and $\rho(\omega_q)$ is the density of states normalized to unit area. For a linear branch, with a sound velocity c, we would have $\omega_q = cq$. It is clear that for low values of Q the amplitude factor A is small and the density of states (which varies initially as ω_q^2) is also small. However, in this limit the product $A\rho(\omega)$ becomes independent of ω if the dispersion is linear [11]. In addition, as the modes in a crystal are expected to be long lived they are represented as δ-functions. For damped modes in an amorphous material they might be represented as Lorentzian functions, with a peak width Γ proportional to Q^2 in the (small Q) hydrodynamic limit. Provided that they have sufficient intensity these peaks are therefore easiest to detect, and their width Γ is smallest at momentum transfers within the first pseudo-Brillouin zone. For a full mixed mode treatment, functions of interest include the symmetrized function $S_1^{sym}(Q,\omega)$ given by [3],

$$S_1(Q,\omega) = \mathrm{e}^{(\overline{h}\omega/2k_BT)}S_1^{sym}(Q,\omega) \tag{6}$$

and the one phonon spectral function $f_1(Q,\omega)$, which can also be calculated directly from theory:

$$f_1(Q,\omega) = \sum_{\alpha\beta}\frac{\mathrm{e}^{-2W}f_{\alpha\beta}(Q,\omega)c_\alpha c_\beta}{\sqrt{M_\alpha M_\beta}} \tag{7}$$

where c_α and c_β are the concentrations of the Mg and Zn and

$$f_{\alpha,\beta}(Q,\omega) = \frac{\omega(1-\mathrm{e}^{(-\overline{h}\omega/k_BT)})}{\overline{h}Q^2}S_{\alpha\beta}^1(Q,\omega) \tag{8}$$

where $S_{\alpha\beta}(Q)$ are the partial dynamic structure factors related to the Mg–Mg, Zn–Zn and Mg–Zn correlations; of these, S_{MgMg} dominates in this experiment (see figure 5). Function (8) is similar to that used in the theory of crystals [10], and a superscript is used here in place of the subscript in equations (2)–(7).

3. Experimental

The $Mg_{70}Zn_{30}$ sample and neutron spectrometer have been previously described in reference [5]. Shortly before this experiment, both x-ray and neutron checks were made on the sample used in [5] to ensure that the glassy nature of the sample was unchanged. This $Mg_{70}Zn_{30}$ sample (of mean density $= 1.72$ g cm^{-3}), was fabricated from high purity elements by melt spinning. The sample container was a flat aluminium alloy vessel of volume 8.0 (height) $\times$ 5.5 (width) $\times$ 2.0 (thick) cm^3 intersected by a square grid of 0.5 mm thick cadmium blades forming multiple cells of 6mm $\times$ 6 mm sides.

This experiment was performed with the sample at 297 K, using epithermal neutrons. An incident beam energy of 0.184 eV (close to the absorption maximum for neutrons in Cd) was chosen to provide a neutron velocity greater than the velocity of sound, and to maximize the absorption of the grid and thereby reduce the (otherwise) large background of multiply scattered neutrons. An identical grid was also used for the empty sample container run, and two halves of the same grid construction were placed at either side of a 3 mm vanadium plate at room temperature for the calibration run. All sets of measurements were carried out under identical experimental conditions and temperature fluctuations were kept to within 3 °C between runs. The sample alignment was set at 4° to the beam, in a plane perpendicular to it.

PHAROS is a direct geometry inelastic chopper spectrometer, ideal for NBS experiments requiring high ω-resolution work. The fast Fermi chopper was run at 467 Hz for these experiments, giving a measured resolution of 4.6 meV FWHM at the elastic line. This chopper frequency was optimum for this instrument. The resolution was a factor of two better than that of our previous experiment using PHAROS [5] at a loss of only half the count rate.

A boron carbide mask defined the incident beam of 7.5 cm $\times$ 5.0 cm at the sample position, and at the time of the experiment the detector grid comprised five banks of linear position sensitive ^{3}He detectors covering 1.3–8.8° in the forward scattering direction. The position sensitivity gave an x–y distribution for the detector cells. The spatial resolution was 2.5 cm in the x- and y-directions. Due to the relatively low flux at high incident energies, low scattering angles and attenuation of the scattered beam by the cadmium grid, a sample run time of 6.5 days at 297 K was required to obtain useful statistics.

The dynamical Q–ω range of the experiment is given in figure 1. This figure shows the range of the low angle detector coverage by full lines, together with theoretical curves from [9] (dashed lines) for the two longitudinal modes in $Mg_{70}Zn_{30}$ glass. The curvature in Q–ω space arising from the limits to the angular range is clearly shown. A locus of constant Q would intersect the solid lines in figure 1 and show the range of energy transfer over which a particular Q could be observed. The pixels of the x–y detector were grouped into constant Q data sets and energy bands of such a width that reasonable counting statistics were obtained and a direct comparison to theory could be made.

4. Analysis of the data

A new software program [12] was employed to group the detector data at constant momentum transfer on the PHAROS instrument. The x–y data were directly binned into constant Q data. In order to compare directly with the theoretical predictions of Hafner [9] identical constant Q cuts were taken at 6.2, 9.4 and 12.6 nm^{-1}†, each with a finite bandwidth of 3.2 nm^{-1}. The program was also used to rebin time-of-flight data to energy transfer data on a linear scale, and provide a correction for neutron capture efficiency in these cylindrical detectors. The data sets

† The theoretical calculations were performed at $Q = 12.5$ nm^{-1} rather than 12.6 nm^{-1}.

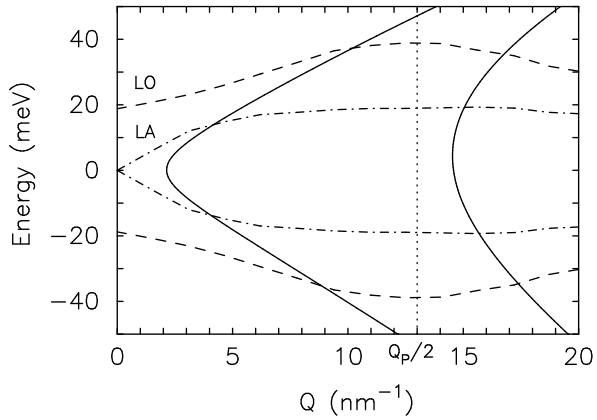

Figure 1. The region in Q–ω space along which x–y data were collected using the low angle detector banks on the PHAROS spectrometer (area between the solid lines). The dashed lines correspond to the theoretical curves for the two longitudinal modes (see text) calculated by Hafner [9] for the metallic glass $Mg_{70}Zn_{30}$. (LA = longitudinal acoustic; LO = longitudinal optic). Also shown is the first pseudo-Brillouin zone boundary $Q_P/2$ (dotted line).

were normalized to the similarly treated vanadium spectra, using the number of counts in the elastic peak of these spectra. The neutron data were corrected for empty container scattering, attenuation and multiple scattering effects (see figure 2). The multiple scattering correction was performed with the help of the Monte Carlo simulation program DISCUS [13] using the measured vibrational density of states from reference [3] as an input model calculation for $S(Q, \omega)$. Corrections for multi-phonon effects (known to be broad in glasses and generally at higher energy transfers) and the finite resolution of the spectrometer were neglected in this analysis.

The symmetrized function $S_1^{sym}(Q, \omega)$ was also evaluated (see equation 6) to ensure that the correct amount of multiple scattering had been subtracted in the data reduction and condition of detailed balance was obeyed, i.e. the plus and minus ω sides should have the same intensity, but the minus side should exhibit a higher resolution. An example of some symmetrized data are shown in figure 3 for $Q = 9.4$ nm^{-1}. The data show a clear division between two modes on the energy loss side of the spectra. In addition, it was noted that the peaks in the structured component $S_1(Q, \omega)$ were broader than the resolution function. This implies either that the excitations are strongly damped or that there are a number of closely spaced sharp peaks. If the excitations were long-lived (i.e. excitation lifetime > 0.1 ps), the latter assumption would be correct.

5. Discussion and conclusions

The improved energy resolution obtained using PHAROS and constant momentum transfer measurements have yielded data which can be compared directly to both our previous experiments and to constant Q theoretical calculations. Thus, the constant Q results obtained here allow a direct comparison to be made with existing theories on the dynamics of $Mg_{70}Zn_{30}$ glass for the first time. The line-shapes and positions of the experimental and theoretical excitations are compared in two representations to emphasise the low and high energy transfer regions. The low energy transfer region is best compared through the function $S_1(Q, \omega)$; this is shown in figure 4, which shows three constant Q plots. Although the data were not explicitly

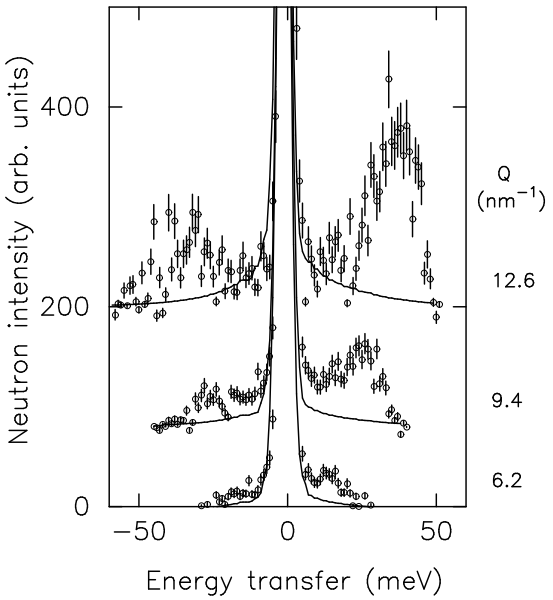

Figure 2. The background corrected inelastic neutron intensity for $Mg_{70}Zn_{30}$ glass (circles with error bars) at three constant momentum transfers $Q = 6.2$ nm^{-1}, $Q = 9.4$ nm^{-1} (shifted by +80), $Q = 12.6$ nm^{-1} (shifted by +200). The solid line represents the elastic line, $S_0(Q, \omega)$, plus the multiple scattering contribution to the measured spectra (see text).

corrected for resolution effects or multi-phonon terms it is assumed that the peaks in figure 5 provide a reasonable measurement of the position and shape of single mode scattering events. In figure 4, comparison of $S_1(Q, \omega)$ from experiment and theory show general disagreements at all three Q values, with the exception of the peak widths and the occurrence of a 40 meV peak at $Q = 12.6$ nm^{-1}. A noticeable discrepancy is the additional peak at low energy transfers predicted by the simulation for $Q = 12.6$ nm^{-1} which is absent in the experimental data.

Usually, the theoretically calculated quantity is the one-phonon spectral function given by $f_1(Q, \omega)$, which emphasises the higher energy transfer region, shifting the peak position up in energy by 2–3 meV compared to $S_1(Q, \omega)$. In our analysis we attempt to extract the same quantity experimentally through equations (2)–(7). The results are shown in figure 5. The theoretical curves have been normalized to the experimental peak heights of the $f_1(Q, \omega)$ function. In this representation both the experimental and theoretical spectral line-shapes and widths are in good agreement; however, the position of the experimental peak at the lower Q values is shifted towards lower energy transfers. The additional feature in the simulation at low energy transfers for $Q = 12.6$ nm^{-1} (which was mentioned previously) is still present but greatly de-emphasised in this representation. From the constant Q results for $Q = 6.2$, 9.4 and 12.6 nm^{-1}, the peak positions (in ω and Q) in $f_1(Q, \omega)$ were read off and have been plotted in figure 6. Suprisingly, the constant Q data points lie on a straight line and do not tend towards the speed of sound curve at low Q. This may be a feature of two modes merging or coupling to give an erroneous dispersion curve. Also shown in this figure are our earlier data on longitudinal modes in $Mg_{70}Zn_{30}$ glass measured at constant angle, and the predicted dispersion curves of the longitudinal optic and acoustic modes by Hafner [9]. The dispersion curves obtained from the constant Q data presented in this paper clearly highlight

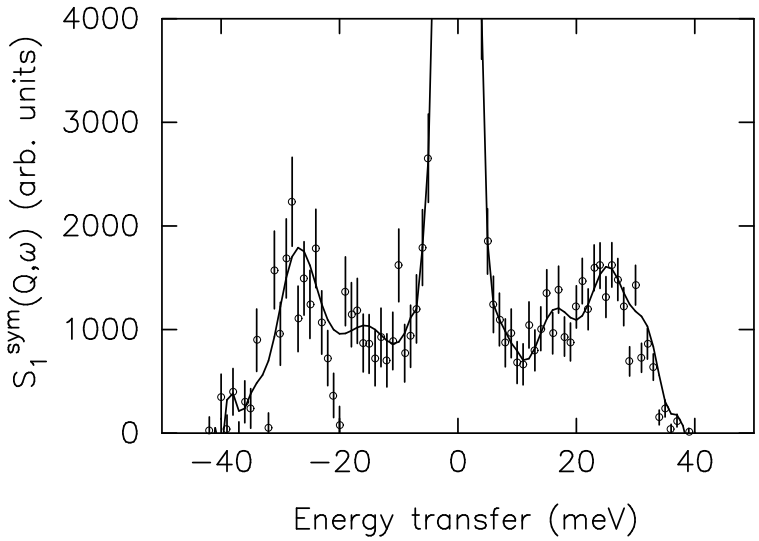

Figure 3. The symmetrized dynamic structure factor $S_1^{sym}(Q,\omega)$ for $Mg_{70}Zn_{30}$ glass at $Q = 9.4\ \mathrm{nm}^{-1}$ (circles and error bars). The solid line was obtained by fitting a high order Chebyshev polynomial to the data points as a guide to the eye.

the problem of comparing structures in $S(Q,\omega)$ and $f(Q,\omega)$ and in the representation of the data at constant angle instead of constant Q curves.

It is expected [9] that only at the lowest momentum transfers ($Q \leqslant 3.1\ \mathrm{nm}^{-1}$) can the acoustic and optic modes be clearly identified. We observe two separate (but undefined) modes at somewhat higher values of Q. For larger Q-values, towards the first pseudo Brillouin zone boundary ($Q \geqslant 6.2\,\mathrm{nm}^{-1}$ in [9]) it has been predicted that the acoustic and optic modes will tend to be dominated by the vibrations of the Zn and Mg atoms, respectively. A comparison of these calculations with the experimental data suggest that the main phonon intensity measured near the first pseudo-Brillouin zone boundary originates from the longitudinal optic mode, which is related to the larger amplitude vibrations of the lighter Mg atoms. However, as Q is decreased the neutron intensity is shifted towards lower energies compared to the simulation. In figure 5 the calculated contribution only from the longitudinal acoustic mode due to the Zn atomic vibrations at $Q = 6.2\ \mathrm{nm}^{-1}$ have been scaled up and plotted, showing reasonable agreement with experiment. One possible explanation for this similarity is that there is a coupling between modes in which the Zn mode is amplified. The measurement at $Q = 9.4\,\mathrm{nm}^{-1}$ is in agreement with our previous data taken at constant angle showing a peak and shoulder on both the energy loss and energy gain sides of the spectra. The principal peak position lies mid-way between the two predicted longitudinal modes suggesting that this may be a combination of modes. If true, this may explain the unexpected experimental dispersion seen in figure 6, especially at the lowest Q value. Unfortunately, the predicted longitudinal one phonon spectral functions from the simulation are inconsistent with the experimental data throughout the first pseudo-Brillouin zone, making mode assignment difficult. Consequently, until the correct mode assignments at each measured Q value can be made unambiguously, the degree to which mode mixing occurs in glassy $Mg_{70}Zn_{30}$ is unclear. For a better understanding of the phonon dispersion in this metallic glass new simulations and higher resolution experiments at smaller momentum transfer intervals are required.

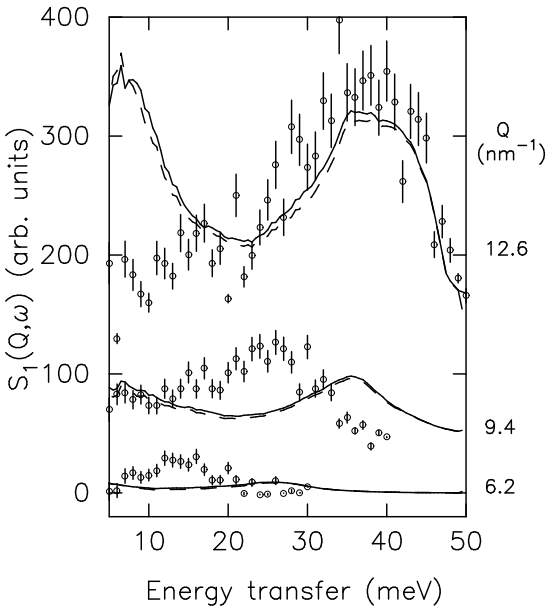

Figure 4. The single excitation part of the dynamical structure factor $S_1(Q,\omega)$ (circles and error bars) for $Mg_{70}Zn_{30}$ glass measured at $Q = 6.2$ nm^{-1}, $Q = 9.4$ nm^{-1} (shifted by +50), $Q = 12.6$ nm^{-1} (shifted by +150). These were obtained assuming the multi-phonon process to be negligible, i.e. $S_m(Q,\omega) = 0$ in equation (2). The lines represent the expected neutron intensity from the theoretical phonon calculations of Hafner [9]. The dashed line is the contribution from the Mg–Mg interactions alone and the solid line includes all three contributions, obtained using equations (6) and (7). The closeness of these two lines is due to the Zn mass being much greater than the Mg mass.

Recently, molecular dynamics simulations have been used to interpret inelastic x-ray scattering in water, and it has been suggested that the mixing of transverse and longitudinal modes may occur at $Q > 4$ nm^{-1} [7]. We note that although transverse modes are forbidden in the first Brillouin zone in the case of crystals, it is probable that transverse and longitudinal mode mixing in the first pseudo-Brillouin zone occurs to some extent in all amorphous systems. Another avenue for further research may be x-ray Brillouin scattering, a new and successful method for studying low Z materials, e.g. [7] (and references herein). However, as yet little work has been carried out on glasses containing heavier elements. Preliminary experiments have shown that the contribution from the tails of the instrumental resolution can make interpretation difficult [14]. Also, the strong absorption at the K- and L-edges of heavier elements and corresponding low inelastic scattering intensity make the access to collective excitations more difficult than for low Z materials†.

In summary, the Neutron Brillouin Scattering technique has been used to measure longitudinal excitations in $Mg_{70}Zn_{30}$ glass at momentum transfers within the first pseudo-Brillouin zone. A comparison of the experimental results with existing theory at constant momentum transfer (in figures 4–6) shows a shift of several meV in the peak position of the neutron intensity, towards lower energies. Evidence for two modes is presented and the possibility of mode mixing is discussed. However, new calculations are required before

† JS has performed a preliminary inelastic x-ray experiment on $Mg_{70}Zn_{30}$ glass in which the inelastic part of the spectra were largely washed out by the strong Lorentzian-like tails of the instrumental resolution function.

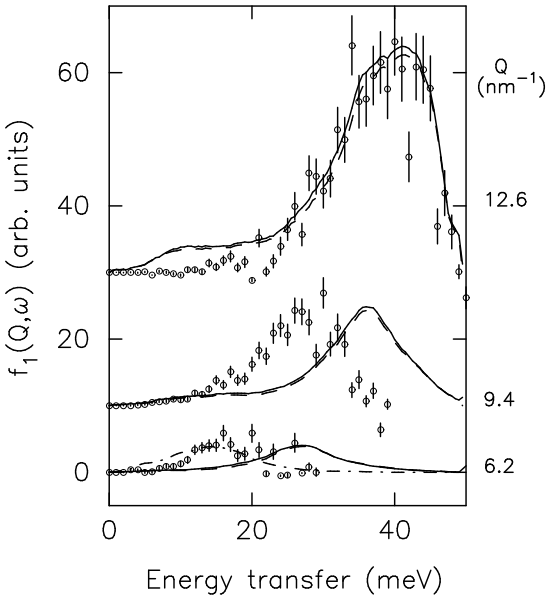

Figure 5. The one-phonon spectral function $f_1(Q, \omega)$ (see equation (7)) for $Mg_{70}Zn_{30}$ glass at 297 K and $Q = 6.2$, 9.4 and 12.5 nm^{-1} emphasising the higher energy transfer part of the spectra. The circles (with error bars) represent the experimental data, whilst the full line represents the theoretical calculations of Hafner [9]. The dashed line represents the contribution of $f_{MgMg}(Q, \omega)$. The single dash–dot line shown for $Q = 6.2$ nm^{-1} is the theoretical contribution of the $f_{ZnZn}(Q, \omega)$ interactions alone scaled by a factor of 15.

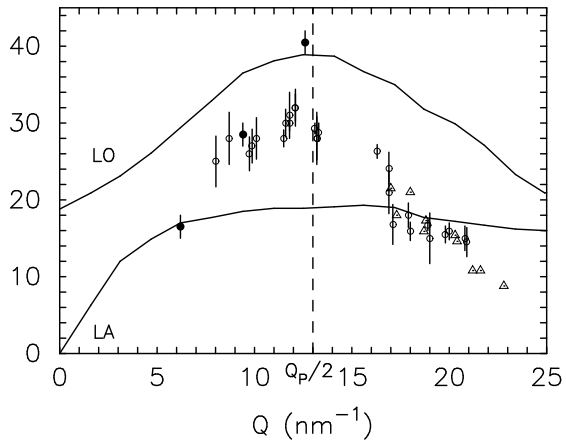

Figure 6. A Q–ω plot for the peaks in $f_1(Q, \omega)$ for the metallic glass $Mg_{70}Zn_{30}$. The results of the present investigation are shown as filled circles for the 297 K data. The open symbols correspond to the previous results on peaks in $S(\theta, \omega)$ on the same metallic glass [1–4]. The solid line corresponds to the theoretical peak positions in $f_1(Q, \omega)$ derived from the calculations of Hafner [9]. The dotted line represents the first pseudo-Brillouin zone boundary $Q_P/2$.

unambiguous mode assignments can be made. It has also been demonstrated that modes can be observed for wavenumbers up to 7 nm^{-1}. Thus, the combination of relatively high

energy inelastic scattering and constant Q analysis of $x-y$ detector data has both extended and improved the experimental work on metallic glasses. Moreover, the way is now open for significant improvements using more advanced instruments on the new generation of high intensity pulsed neutron sources.

Acknowledgments

We would like to acknowledge the assistance of the staff at LANSCE during the course of our experiments. We are also grateful to NSERC of Canada for their financial support of the Canadian participants. This work was funded in part by the division of Basic Energy Science of the US Department of Energy.

References

[1] Suck J-B, Egelstaff P A, Robinson R A, Sivia D S and Taylor A D 1992 *J. Non-Cryst. Solids* **150** 245
[2] Suck J-B, Rudin H, Guntherodt H-J and Beck H 1983 *Phys. Rev. Lett.* **50** 49
[3] Suck J-B, Rudin H, Guntherodt H-J and Beck H 1981 *J. Phys. C: Solid State Phys.* **14** 2305
[4] Suck J-B, Egelstaff P A, Robinson R A, Sivia D S and Taylor A D 1992 *Europhys. Lett.* **19** (3) 207
[5] Benmore C J, Olivier B J, Suck J-B, Robinson R A and Egelstaff P A 1995 *J. Phys.: Condens. Matter* **7** 4775
[6] Benmore C J, Sweeney S, Robinson R A, Egelstaff P A and Suck J-B *Physica* B **241** 912
[7] Sampoli M., Ruocco G and Sette F 1997 *Phys. Rev. Lett.* **79** 1678
[8] Robinson R A 1989 *Advanced Neutron Sources (Inst. Phys. Conf. Ser., Topics in Applied Physics)* **97** 311
[9] Hafner J 1983 *J. Phys. C: Solid State Phys.* **16** 5773
[10] Squires G L 1978 *Introduction to the Theory of Thermal Neutron Scattering* (Cambridge: Cambridge University Press)
[11] Suck J-B 1993 *Int. J. Mod. Phys.* B **7** 3003
[12] Sweeney S and Benmore C J 1997 Unpublished results
[13] Johnson M W 1974 *DISCUS, A Computer Program for the Calculation of Multiple Scattering Effects in Inelastic Neutron Scattering Experiments* UKAEA Harwell report AERE-R7682
[14] Benassi P, Krisch M, Masciovecchio C, Mazzacurati V, Monaco G, Ruocco G, Sette F and Verbeni R 1996 *Phys. Rev. Lett.* **77** 3835–8